Phase Inversion in Compatibilized Immiscible Polymer Blends with Exothermic Interfacial Mixing

Adeyinka Adedeji, Alex M. Jamieson,* and Steven D. Hudson

Department of Macromolecular Science, Case Western Reserve University, Cleveland, Ohio 44106

Received February 7, 1995; Revised Manuscript Received May 11, 1995[⊗]

ABSTRACT: We have investigated the morphology of solvent-cast immiscible polymer blends, emulsified by block copolymers that exhibit exothermic interfacial mixing. By manipulating the balance between core and corona swelling, we generate a variety of new microstructures. Specifically, it is demonstrated that the minor component becomes the continuous phase when the core swelling is sufficiently large by a process of vesicle fusion which produces an interconnected phase-inverted network morphology. This phenomenon was observed in blends of poly(styrene-*co*-acrylonitrile) (SAN) with polystyrene (PS) emulsified with poly(methyl methacrylate-*b*-styrene) (PMMA-*b*-PS). The degree of exothermic mixing between SAN and the PMMA block was varied by changing the AN content of SAN. In blends where SAN is the minor component, the core swelling increases on decreasing AN content, while the corona swelling in the PS major phase is determined by the molecular weight of the block copolymer PS segment relative to that of the matrix. For a particular combination of molecular weights of the blend components, by decreasing the AN content of SAN, we produce microstructural transformations from isolated vesicles to fused vesicles and finally to the phase-inverted network. Exothermic swelling maximizes the interfacial area of the minor phase and tends to yield planar interfaces, without sacrificing high molecular weight. Thus, the minor phase domains are stable against rupture and form the continuous phase. When SAN is the major component, the same tendency leads to a loss of emulsifying effectiveness because of the extremely small particle sizes of the disperse PS phase.

Introduction

Binary mixtures of block copolymers with homopolymers can form a rich variety of microstructures including spherical and cylindrical micelles, vesicles, ordered bicontinuous double diamond, gyroid, catenoid lamellae and planar lamellae.[1–11] These microstructures are the result of the spontaneous interfacial areas and curvatures that are established at equilibrium. The average interfacial curvature is highest for spheres and decreases progressively toward planar interfaces in lamellae.[2,9,10] Generally, spherical micelles are formed when a segment A of a symmetric diblock copolymer A-*b*-B is strongly solubilized by homopolymer A and the block segment B, immiscible with A, forms the microdomain. In such isochemical blends, the homopolymer A swells the surface of the block copolymer only when the molecular weight of the homopolymer A is lower than or equal to that of the block segment A.[3–7,9,10,15] The interfacial region defined by the block segment A brush with solubilized homopolymer A is generally referred to as the corona, and the microdomain that contains segment B, as the core. As the swelling of block A by homopolymer A decreases, the corona volume decreases and less curved interfaces are formed. When the interfacial curvature is negligible, we find planar interfaces, e.g., lamellae.[2,3,6,7,9,10] Corona volume depends on the degree of swelling of the block copolymer brush and should, therefore, be influenced by any factor that can modify the corona wetting. In addition to lowering the homopolymer molecular weight with respect to that of the compatible block segment,[3–7,9,10,15] this could also include introducing exothermic mixing between homopolymer A and block segment X in A/X-*b*-B blends.[13,14,21–23] Specifically, as the degree of exothermic mixing decreases, the corona volume will decrease and generate a more planar interface.

In ternary blends containing a diblock copolymer (i.e., A/A-*b*-B/B), the overall interfacial curvature is determined by the balance between interfacial swelling of the block copolymer segments on both sides of the interface. Again the degree of swelling may be manipulated by varying the molecular weights of the homopolymer A and B relative to those of the block segments A and B[15] or by choosing chemistries of the blend constituents in a fashion that they will produce exothermic interfacial mixing as in A/X-*b*-Y/B blends. Here, we describe morphological transformations in blends of the type A/X-*b*-B/B, with exothermic mixing between A and X.[13,16,17] We further present evidence that these microstructural transformations can be interpreted in terms of the relative swelling activities on each side of the interface. The interfaces are curved when swelling on one side is larger than on the other and become planar when the swelling on both sides is comparable.[3,9,18,31]

Inverse Morphology. Diblock copolymers exhibit spherical (body-centered cubic), cylindrical (hexagonal packing), and lamellar morphologies,[2,12,19,25–27,31] depending on their composition variable, *f*. For example, poly(styrene-*b*-butadiene) (SB) with *f* less than 15% weight fraction of the styrene block forms spheres of styrene in a matrix of butadiene; when $f = 15–35$ wt %, SB forms cylinders of styrene in a butadiene matrix; lamellae are formed when $f = 35–65$ wt %.[28] On further increasing *f*, a reverse of the morphological trend is observed as cylinders and spheres of the butadiene are formed in a matrix of styrene at $f = 65–85$ wt % and $f > 85$, respectively.[28] In addition, in binary mixtures of homopolymers with block copolymers, the major component forms the continuous phase and the minor component forms the discrete phase. When the volume fraction of the major component is decreased so that it becomes the minor component, this species, which previously existed as the continuous phase, becomes the discrete phase. Specifically, Winey et al.[29] have demonstrated experimentally that the addition of polysty-

[⊗] Abstract published in *Advance ACS Abstracts,* June 15, 1995.

0024-9297/95/2228-5255$09.00/0

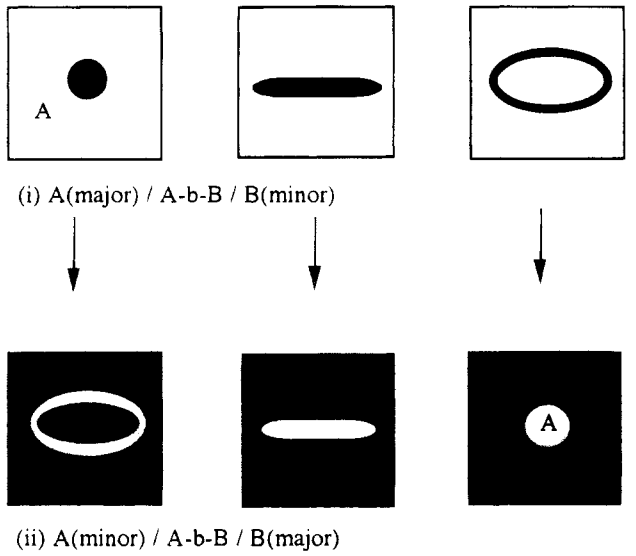

Figure 1. Microstructural transformation on inverting the composition of the constituent polymers. The B component is represented as the dark portion. This diagram is meant to illustrate general trends rather than specific one-to-one correspondence as indicated by the arrows.

rene (PS) homopolymer to neat poly(styrene-*b*-butadiene) or poly(styrene-*b*-isoprene) (PS volume fraction ranges from 44 to 51%) produces an isothermal morphological transition from a cylindrical to spherical polybutadiene or polyisoprene microphase. In addition, such morphological transitions can also be induced by modulating the molecular weight of the homopolymer relative to that of the compatible bcp segment. In particular, in solvent-cast blends of polystyrene (PS) with poly(styrene-*b*-butadiene) (SB) as shown by Kinning et al.,[6] when 12.5 wt % of an SB copolymer (M_w = 20Kd-*b*-20Kd) was mixed with PS (M_w = 2100, 3900, or 7400), only spherical micelles of the polybutadiene block were formed, whereas, with PS (M_w = 17 000), cylindrical micelles were observed. Moreover, vesicular micelles were observed in a mixture of 5.0 wt % of an SB copolymer (M_w = 40Kd-*b*-40Kd) with PS (M_w = 35 000), where the M_h/M_b ratio is close to unity. It was pointed out that, since the diameters of the vesicles are much larger than their thicknesses, vesicular curvature is very small and essentially lamellar in nature.[6] This morphological trend corresponds to that sketched diagrammatically in Figure 1i.

Similarly, in ternary A/A-*b*-B/B blends, when homopolymer A is the major component, it forms the continuous phase, whereas homopolymer B as the minor component forms the core microdomains. The microstructure of the disperse B phase is expected to transform from spheres to cylinders and then to vesicles as the core volume increases and counteracts that of the corona (A/A swelling). This is depicted in Figure 1i. Note that the core volume can be increased by increasing the volume fraction of B component via an increase in the block copolymer volume fraction; by increasing the B block length relative to that of the A block; by increasing the homopolymer B volume fraction; by increasing the B/B swelling through lowering of the M_{hB}/M_{bB} ratio; by decreasing the A/A swelling through increasing the M_{hA}/M_{bA} ratio; or by introduction of a homopolymer that has an exothermic interaction with the B block. Here, M_{hA} is the molecular weight of homopolymer A, and M_{bA} is that of block A of the block copolymer. If the molecular weights and the chemistries of the blend constituents are unchanged, it is expected that a spherical microphase of B will transform to a vesicular microphase of A when the blend composition is inverted, i.e., changed to A(minor)/A-*b*-B/B(major) because the strong A/A swelling activity is now in the core. Likewise, cylinders of B will transform to cylinders of A and vesicles of B to spheres of A. This process is schematically shown in Figure 1ii. In each case, the new microstructures are generated because inversion of the blend composition interchanges swollen locations.[19,20]

In this study, we investigate the morphology of immiscible blends of poly(styrene-*co*-acrylonitrile) (SAN) and homopolymer PS compatibilized with PMMA-*b*-PS, in which the swelling of the PMMA block segment can be systematically varied through changes in the acrylonitrile (AN) content of SAN which produces variation in the extent of exothermic mixing between SAN and PMMA. We explore examples where the exothermic swelling occurs in the corona (when SAN is the major phase) and where it occurs in the core (when SAN is the minor phase). Our observations uncover new morphological features in addition to the expected transition from spherical to cylindrical and vesicular micelles. Specifically, we find that an increase in swelling of the core can lead not only to formation of vesicles but also to a further process of vesicle fusion and eventually to complete phase inversion; i.e., the minor component becomes the continuous phase.

Experimental Section

Materials. Polymers used for this investigation were 680Kd PMMA-*b*-PS (220Kd:460Kd, M_w/M_n = 1.10), henceforth designated B(680), from Polysciences Inc. This copolymer forms a lamellar microstructure in the melt. Its molecular weight is sufficiently large that its disordering temperature would be inaccessibly high. PS (90Kd, M_w/M_n = 1.04) and PS-(105Kd, M_w/M_n = 1.06) were from Pressure Chemical Co., and SAN with 15, 26, 29, or 33% AN content (163, 153, 151, 130Kd, M_w/M_n = 2.12, 2.16, 2.23, 1.95)[24] were supplied by Mitsui Toatsu Chemicals Inc. The SANs will hereafter be referred to as SAN15, SAN26, SAN29, and SAN33, where the last two numerals indicate the percentage of AN.

Sample Preparation. Stock solutions of each of these polymers were made at room temperature in methyl ethyl ketone (MEK) at a concentration of 1 g/100 mL. Each blend contains 77.5 v/v % of the SAN or PS solution, 15 v/v % of the PMMA-*b*-PS, and 7.5 v/v % of the PS or SAN. Blend solutions containing PS(90Kd) were cast on a clean mercury surface, in 12 × 75 mm Pyrex test tubes; blend solutions containing PS-(105Kd) were cast on the glass surface of similar test tubes. The solvent was slowly removed at room temperature over 7 days. Final traces of the solvent were removed by drying at 70 °C for 1 day at atmospheric pressure and then for 1 day under vacuum. The samples were further annealed just above the T_g (105 °C) for 5 days under vacuum.

Transmission Electron Microscopy. Central portions of the cast films (~0.2–0.4 mm thick) were sectioned, using a diamond knife, with a RMC Inc. MT-7000 ultramicrotome machine in a direction normal to the surface to obtain thin films (70–90 nm thick). The films were scooped from the water surface with uncoated 3 mm standard copper grids and were poststained with RuO_4 vapor for 45 min in an enclosed chamber containing about a 0.15% aqueous solution of RuO_4. The PS component is stained by RuO_4. Bright-field images were obtained by mass–thickness contrast on a JEOL JEM-100SX, transmission electron microscope, at an accelerating voltage of 100 kV. PS appears as the darkest regions in the TEM micrographs since the SANs and PMMA are only lightly stained.

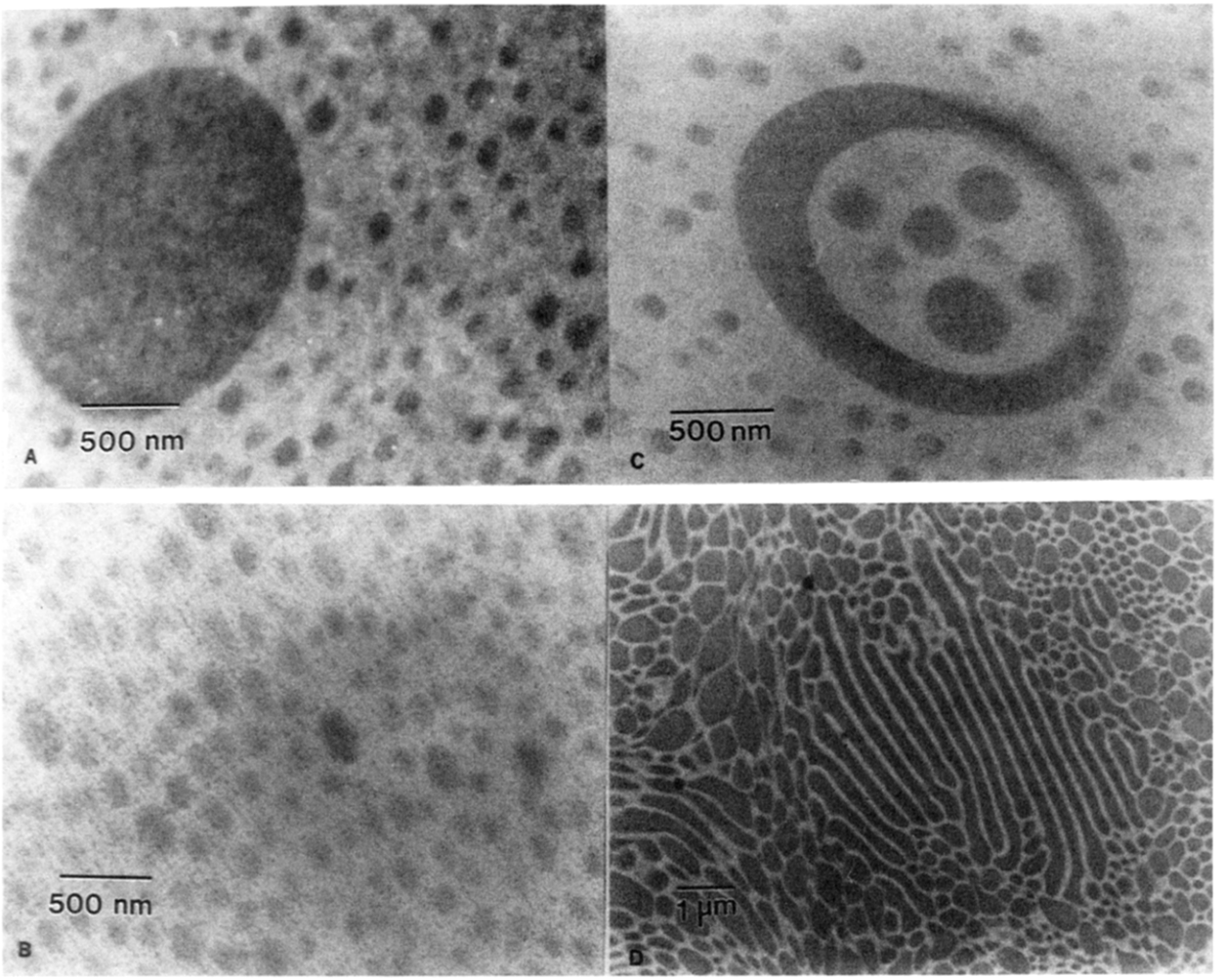

Figure 2. Microstructural transformation from spherical micelles coexisting with the PS macrodomain to only spherical, spherical and vesicular, and spherical and elongated micelles in SAN/B(680)/PS(90): (A) SAN15; (B) SAN26; (C) SAN29; (D) SAN33.

Results

When SAN is either the minor or the major component of the blends, there is a systematic change in the morphological microstructures as the degree of exothermic mixing between the SAN and the PMMA block is varied. Electron micrographs of SAN/PS-*b*-PMMA(680Kd)/PS(90Kd) blends where SAN is the major component are shown in Figure 2a–d in order of increasing AN content of SAN. For blends with higher AN content, as evident in parts b–c of Figure 2, microphase separation only is observed. Macrophase separation occurred upon solution casting of the blend containing SAN33, as discussed in more detail later. Shown in Figure 2d is a PS-rich region. Interestingly, as seen in Figure 2a, macrophase separation also occurs at the lowest AN content when exothermic mixing is greatest (SAN15). The microdomain interfaces become more planar on decreasing the degree of exothermic mixing in the corona. This is manifested by the appearance of vesicles in blends containing SAN29 (Figure 2c) and elongated micelles in blends containing SAN33 (Figure 2d).

Parts a–d of Figure 3 show the inverse morphology of SAN/PS-*b*-PMMA(680Kd)/PS(90Kd) blends where PS(90Kd) is the major component and SAN is the minor component, in decreasing order of the AN content of SAN. Here we find a quite different morphology which indicates a trend toward phase inversion with decreasing AN content of SAN, i.e., as the exothermic mixing in the core increases. Thus, in the blend containing SAN33 (Figure 3a), we observe many isolated vesicles and elongated micelles; in SAN29 and SAN26 we see an increasing trend toward vesicle fusion (Figure 3b,c); and, finally, in SAN15 (Figure 3d) we find complete phase inversion and formation of an interconnected polygonal network morphology. Parts a–d of Figure 4 show the morphologies of blends of identical composition but with PS(105Kd) as the major component. Apparently, a small increment of the PS homopolymer M_w is sufficient to produce phase inversion for all four SAN polymers. Interpretation of the morphological transition in each blend is discussed below in detail.

Discussion

In SAN/PMMA-*b*-PS/PS blends, where SAN is the major component, exothermic mixing between SAN and the PMMA block segment occurs in the corona; the PS minor component forms the core of the micelles. As the degree of SAN/PMMA exothermic mixing decreases as the AN content increases, we see a transformation in the microstructure from spherical microdomains coexisting with a few PS macrodomains in the SAN15 blend (Figure 2a) to only spherical microdomains in the SAN26 blend (Figure 2b), to spherical and vesicular micelles in the SAN29 blend (Figure 2c), and spherical and elongated micelles in SAN33 (Figure 2d). Note that the molecular weight ratio of SAN to PMMA block decreases from 0.74 for SAN15 to 0.60 for SAN33. This will produce a small increase in the wetting of the

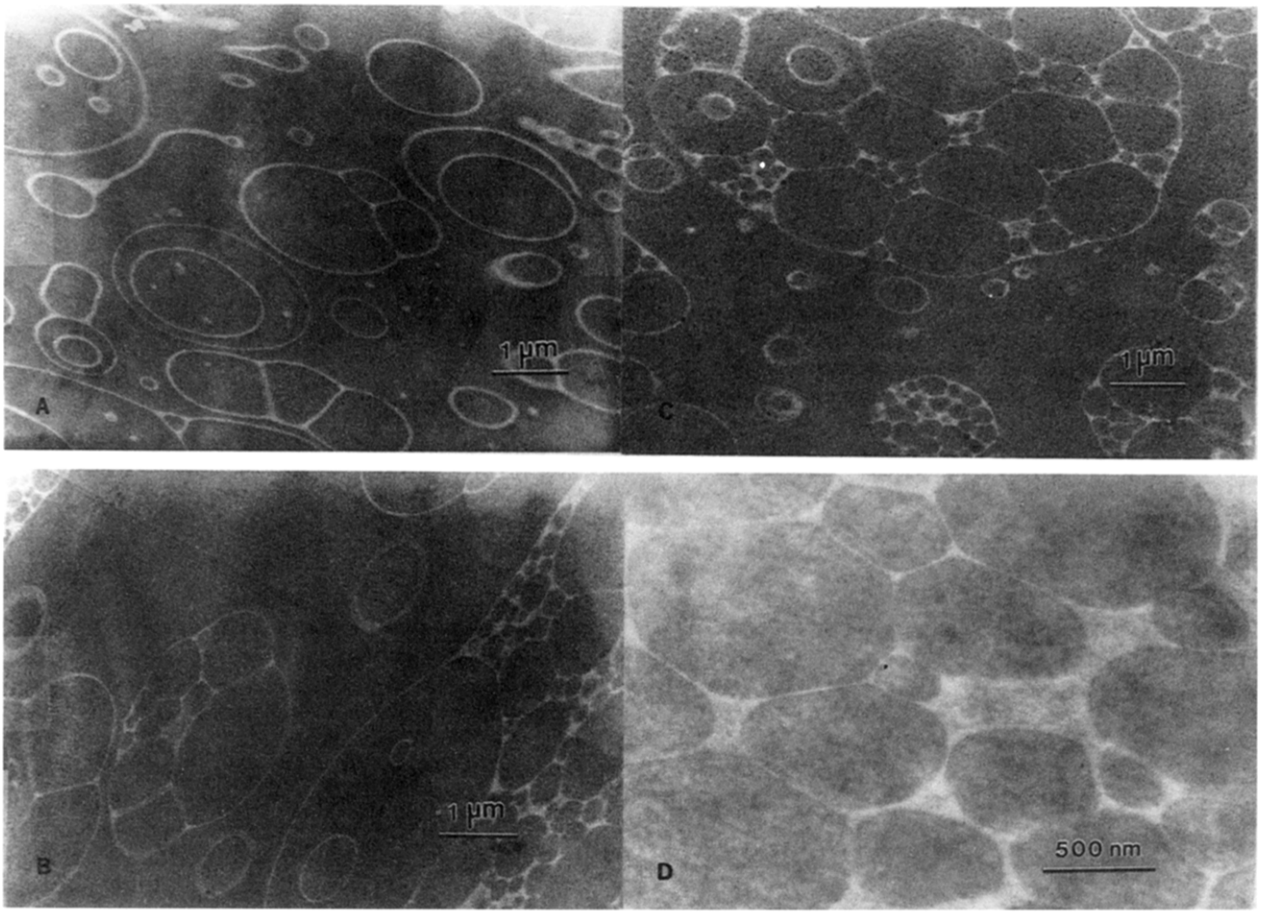

Figure 3. Microstructural transformation in PS(90)/B(680)/SAN, when the exothermic mixing is in the core: (A) SAN33; (B) SAN29; (C) SAN26; (D) SAN15.

PMMA corona as AN increases, i.e., an effect which runs counter to that produced by the exothermic mixing. We will argue, therefore, that the results shown in Figure 2 cannot be explained in terms of molecular weight ratios.

The coexistence of spherical micelles and the macrophase of PS in the SAN15 blend can be rationalized as an example of "emulsification failure" described by Wang and Safran[18] when there is very strong wetting of the micellar corona and hence a very large interfacial area (small disperse phase sizes). This effect is attributed to an insufficient amount of block copolymer to completely emulsify the homopolymer present in the blend. We, therefore, interpret the observed phenomenon to be attributable to the very strong swelling of the PMMA block segments by the SAN15[17] which increases the interfacial area density of the block copolymer chains and induces a core volume reduction via rearrangement of the core chains so as to maintain a constant core chain density that is similar to that of the pure homopolymer. This core volume reduction reduces the capacity of the PS homopolymer that can be accommodated in the core; hence, the excess PS homopolymer is observed as macrodomains. Thus, a strong exothermic swelling of a block copolymer segment in a micellar corona may reduce the emulsifying power of the block copolymer, and since the strength of this swelling is proportional to $\chi_{AX}N_X$, even small values of χ_{AX} can lead to significant corona swelling. Note that the spherical micellar domains in Figure 3a are much larger than those expected to be formed by mutual association of the block copolymer chains only. To see this, we compare the average spherical domain size with the radius of gyration (R_g) of the PS block segment. Assuming a Gaussian coil,[30] R_g of the PS block segment of B(680) is estimated to be 18.7 nm, whereas the experimental diameter of the spherical domains in Figure 3a is 140 nm. Hence, we can safely conclude that the spherical domains do indeed contain emulsified PS homopolymer and that the presence of a PS macrophase in the SAN15 blend is an example[18] or emulsification failure.

In the SAN26 blend where there are no PS macrodomains, the average core diameter increases to an average of 160 nm. This increment in the microdomain size can be attributed to an increase in emulsifying effectiveness of the block copolymer due to a decrease in the SAN/PMMA exothermic mixing and an accompanying increase in SAN/PS repulsion. Thus, the increase in the spherical domain diameter is due to the increased capacity of the microdomain to accommodate PS homopolymer, explaining the absence of PS macrodomains. The SAN29 blend shows spherical micelles (with a further increase in the average domain diameter to 255 nm) and also a few vesicles. The appearance of vesicles is attributed to the lower degree of exothermic mixing between SAN29 and the PMMA block which reduces the swelling in the corona. The larger size of the spherical micelles inside the vesicle compare to those that are outside suggests to us that macrophase separation may have preceded micelle formation. The tendency to macrophase separate is magnified by increasing the AN content to 33%, since the repulsion between SAN and PS increases while the exothermic mixing between SAN and PMMA decreases. By visual observation, coexistence of turbid and transparent regions

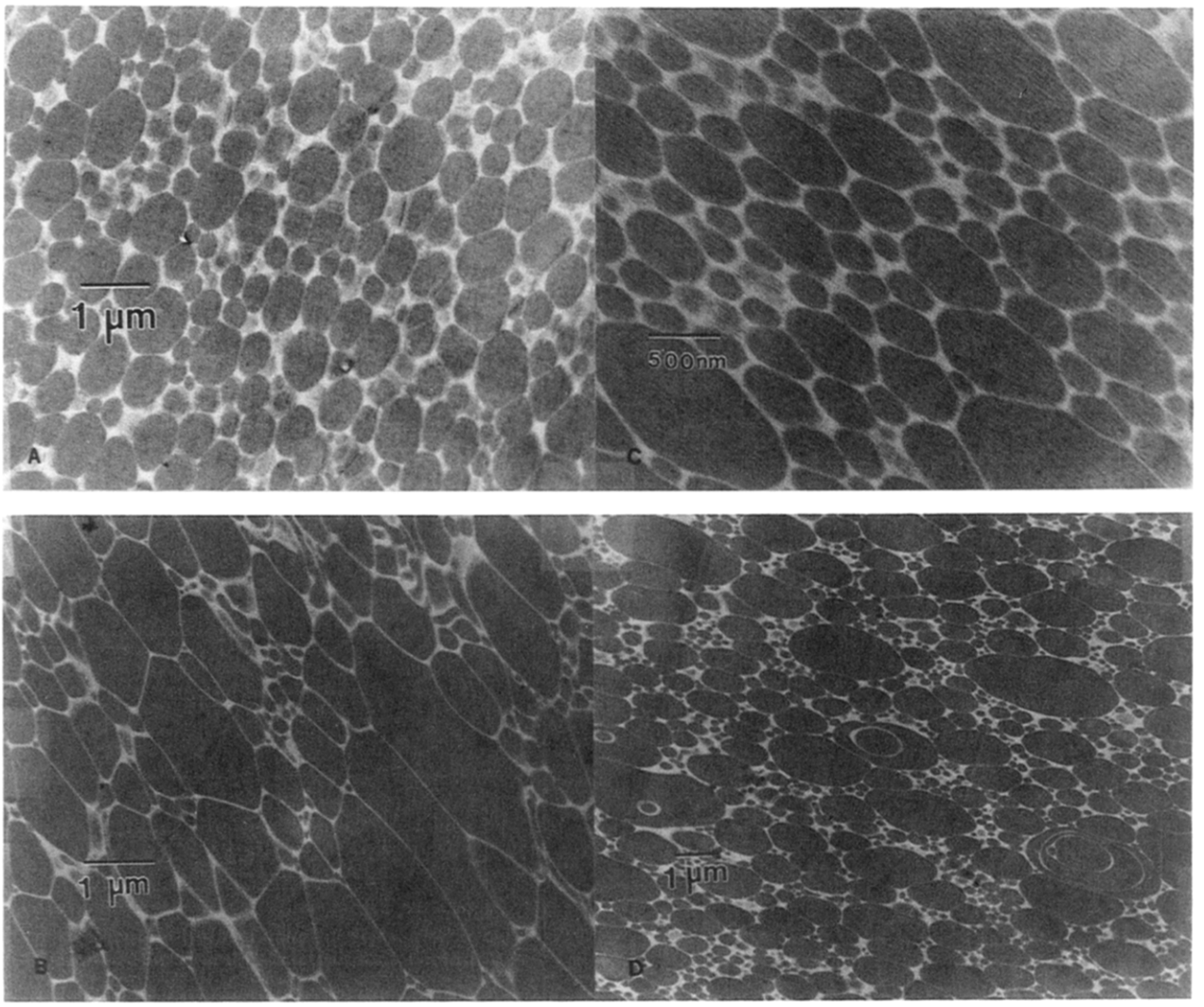

Figure 4. Interconnected polygonal network structures formed at all levels of AN content in SAN by increasing the M_w of the PS homopolymer from 90Kd in 105Kd in PS(105)/B(680)/SAN: (A) SAN15; (B) SAN26; (C) SAN29; (D) SAN33.

was observed in the thick film (ca. 1 mm) of SAN33/PMMA-*b*-PS(680)/PS(90). The transparent and the turbid regions were isolated and examined microscopically. The transparent region showed a homogeneous phase, while the turbid region contained microstructures with very high PS concentration. Apparently, the product χ_{SAN-PS} has become large enough that macrophase separation occurs initially in the casting process, followed by microphase separation.[32] A similar segregation phenomenon was observed for blends containing PS(100), however, with some change in the morphology of the PS-rich macrophase. The micrograph shown in Figure 2d is the morphology of a turbid region in the SAN33/PMMA-*b*-PS(680)/PS(90) blend. Because of the relatively high PS concentration in this region the ratio of dark to bright areas is higher than computed from the overall PS blend composition. The morphology shows some apparently spherical micelles coexisting with elongated structures.

On interchanging the compositions of the constituent polymers, whereby the SANs and the PMMA block segment constitute the core, we observe a systematic morphological trend toward phase inversion with decreasing the AN content of SAN, as displayed in Figure 3. These observations, which were described previously in a preliminary paper,[16] are, to our knowledge, the first reports of such an effect, which arises when the swelling of the core is larger than the corona swelling. In Figure 3a, for the SAN33 blend, when the exothermic mixing or core swelling is minimal, isolated vesicles with a few fused vesicles are formed. On increasing the core swelling by increasing the exothermic mixing between SAN and the PMMA block (i.e., SAN29/PMMA), predominantly fused vesicles are formed with few individual vesicles (Figure 3b). At 26% AN, when the core swelling is further increased, a greater degree of vesicle coalescence occurs to create regions where the minor component (SAN26/PMMA) becomes the continuous phase (Figure 3c). Within this locality, the continuous phase frequently consists of nearly planar membranes enclosing large PS domains. Such planar membranes are also observable in the interior of the fused vesicle domains in parts a and b of Figure 3. At maximal exothermic mixing in the core (SAN15), we find complete phase inversion to form an interconnected polygonal network structure in which the SAN15 phase is the continuous phase (Figure 3d).

Figure 4 demonstrates that it is possible to induce phase inversion at all levels of AN content by increasing the molecular weight of the PS homopolymer from 90 000 to 105 000. This corresponds to a very small increase in the ratio M_h/M_b on the PS side of the interface from 0.20 to 0.23, indicating a rather delicate balance in the interfacial swelling potential. In these blends, recall that a reduction of swelling on the major

component side should indeed favor the phase inversion process.

The observed phase inversion clearly deviates from expectations,[20,28] depicted in Figure 1, regarding the morphological changes which might be induced by inverting the blend composition, while keeping the interfacial swelling tendencies constant. Our observations show that, if we start with a spherical core and increase swelling in the core, vesicles are not the ultimate microstructure that can be generated. Instead, the vesicles can fuse, producing a local phase inversion that grows until the major component forms the discrete phase everywhere, with the minor component becoming the continuous phase. Finally, it is observed that, at locations where the minor SAN phase forms a thin membrane between PS domains, the interfaces are planar. Such planar interfaces are also observed at the boundary between the fused vesicles. This phenomenon is commonly observed in soap bubbles but is unusual in the morphology of emulsified immiscible polymers. In soap bubbles, a network is formed by thin films of a solution of soap and water which enclose pockets of air. Similarly, in the morphology of these blends, a thin membrane consisting of SAN bounded by block copolymer encloses domains of PS. Hence, the foamlike morphology of the blend SAN/PMMA-*b*-PS/PS may be viewed as analogous to soap bubbles in which SAN replaces water, block copolymer replaces the surfactant, and PS replaces air. Further, when a foam is suspended in air, the entrapped water drains to the lower portion and the membranes in the "dry" upper portion become planar, while, in the lower portion which accumulates excess water ("wet" foam), the pockets of air are small in size and spherical in shape. Note that the network morphology in the SAN15/PS-*b*-PMMA(680Kd)/PS(105Kd) blend (Figure 4a) and that in the SAN33/PS-*b*-PMMA(680Kd)/PS(105Kd) blend (Figure 4d) are different and appear analogous to dry and wet soap foams, respectively. We point out that a decrease in the concentration of SAN33 or addition of more block copolymer to the blend shown in Figure 4d should produce a reduction in the amount of excess SAN33, transforming the wet foam into a dry foam. This expectation will be tested in our future work.

The foamlike morphology is not an equilibrium structure and may be viewed as a result of the three-dimensional fusion of vesicles. Figure 5 schematically illustrates the coalescence of two vesicles, leading to formation of stable fused vesicles, separated by a planar membrane wall. Vesicle coalescence of this nature, in three dimensions, leads to a foamlike structure. However, if the membrane wall is unstable, it will break down and a larger vesicle will be formed, as also illustrated in Figure 5. Further, if the new vesicle is itself unstable, it may transform to a planar micelle.

The driving force for vesicle coalescence is to reduce interfacial curvature. Breakup of the vesicle membrane involves formation of a pore through the minor phase. Two factors appear to be important. The first is the thermodynamics of pore formation; when the balance of swelling favors the minor phase, the osmotic pressure resisting pore formation is larger. The second factor is the kinetics of pore formation; if either phase is highly viscous, pore formation is retarded. Lateral entanglements between copolymer chains should be especially effective in maintaining membrane integrity. Our experiments suggest that both factors are important. The thermodynamic effect is clearly manifested in

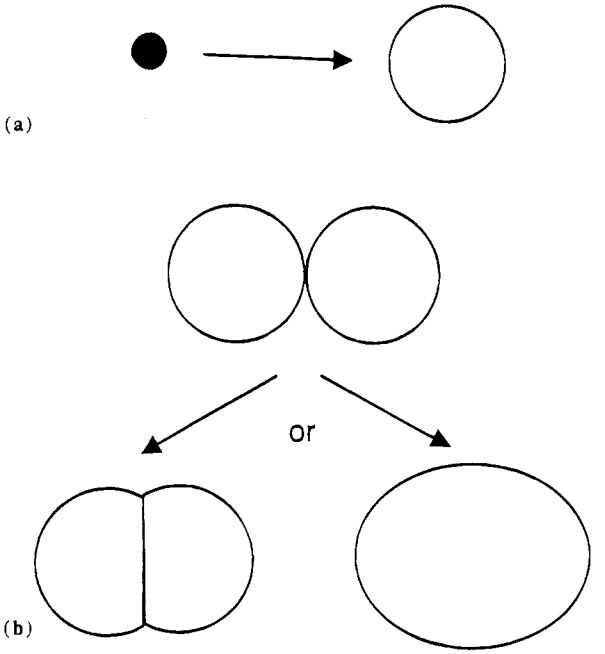

Figure 5. (a) Strong swelling in the core causes the morphology of the minor phase to be vesicular. (b) Depending on the membrane elasticity, stable coalesced vesicles or a larger vesicle can be formed. Strongly interacting high molecular weight homopolymer and high molecular weight block copolymer segments in the core contribute to membrane elasticity and stability, while low molecular weight homopolymer dilutes the entanglement density of the block copolymer chains and lowers the membrane elasticity and stability.

Figure 3; viz., a systematic decrease in exothermic mixing between the PMMA block and the SAN, i.e., a decrease of swelling in the minor phase, leads to a morphological trend toward isolated vesicles. In addition, the molecular weight of all polymers in these blends is well above the entanglement molecular weight. This latter issue will be explored in a future publication.

The phase-inverted morphology itself is not new. It is found on a local scale in high-impact polystyrene (HIPS).[33] However, it is a novel morphology for a blend of linear polymers. In HIPS, polystyrene is the discrete phase and a cross-linked, rubber-rich continuous phase is formed by polymerization. The rubber is prevented from forming a fully-continuous phase by stirring during reaction.[33] As expected, in the present blend system, SAN 15/PS-*b*-PMMA/PS, the fully-interconnected morphology shown in Figures 3d and 4 can be broken up by shear deformation in the melt (~60% strain, 140 °C, frequency = 0.1−100 rad/s).[34] As in HIPS, however, local phase inversion of the minor component remains.

Conclusions

We have carried out morphological studies of the emulsifying effectiveness of a block copolymer in immiscible blends in the presence of an exothermic interfacial interaction. These experiments were performed in PS/PS-*b*-PMMA/SAN blends in which the exothermic interaction between PMMA and SAN is systematically increased by decreasing the AN content of SAN. We confirm earlier observations that the magnitude of the exothermic interaction influences the observed morphology. Blends in which SAN is the major component show a systematic structural transformation from spherical microdomains coexisting with macrodomains of PS homopolymer (SAN15) to only spherical microdomains (SAN26); to coexisting spherical and vesicular micro-

domains (SAN29); and finally to a mixture of spherical and elongated microdomains. These morphological transformations are accompanied by a progressive increase in the diameter of the spherical microdomains. Our observations are consistent with a decrease in the coronal swelling with increasing the AN content of SAN. The presence of a macrophase in SAN15 blends where the coronal swelling is maximal is an example of emulsification failure due to a severe reduction of the micellar core volume. For blends where SAN is the minor component, we observed vesicles and fused vesicles (SAN33), local phase inversion (SAN29 and SAN26), and finally global phase inversion to form an interconnected network (SAN15). Planar interfaces are observed within the phase-inverted regions. This phase-inverted network is stabilized apparently by strong swelling within the minor phase and sufficient copolymer entanglements.

Acknowledgment. We are pleased to acknowledge financial support from the National Science Foundation through Material Research Group award DMR 01845.

References and Notes

(1) Thomas, E. L.; Winey, K. I. *Proc. ACS Div. Polym. Mater. Sci. Eng.* **1990**, *62*, 686.
(2) Hasegawa, H.; Tanaka, H.; Yamasaki, K.; Hashimoto, T. *Macromolecules* **1987**, *20*, 1651–1662.
(3) Mayes, A. M.; Olvera de la Cruz, M. *Macromolecules* **1988**, *21*, 2543–2547.
(4) Spontak, R. J.; Smith, S. D.; Ashraf, A. *Macromolecules* **1993**, *26*, 5118–5124.
(5) Koizumi, S.; Hasegawa, H.; Hashimoto, T. *Makromol. Chem., Macromol. Symp.* **1992**, *62*, 75–91.
(6) Kinning, D. J.; Winey, K. I.; Thomas, E. L. *Macromolecules* **1988**, *21*, 3502–3506.
(7) Winey, K. I.; Thomas, E. L.; Fetters, L. J. *Macromolecules* **1991**, *24*, 6182–6188.
(8) Lowenhaupt, B.; Hellmann, G. P. *Polymer* **1991**, *32*, 1065.
(9) Winey, K. I.; Thomas, E. L.; Fetters, L. J. *J. Chem. Phys.* **1991**, *95* (12), 9367.
(10) Kinning, D. J.; Thomas, E. L.; Fetters, L. J. *J. Chem. Phys.* **1989**, *90* (10), 5806.
(11) Winey, K. I.; Thomas, E. L.; Fetters, L. J. *Macromolecules* **1992**, *25*, 422–428.
(12) Thomas, E. L.; Anderson, D. M.; Henkee, C. S.; Hoffman, D. *Nature* **1988**, *334*, 598.
(13) Akiyama, M.; Jamieson, A. M. *Polymer* **1992**, *33* (17), 3582–3592.
(14) Siqueira, D. F.; Nunes, S. P. *Polymer* **1994**, *35* (3), 490.
(15) Lowenhaupt, B.; Hellmann, G. P. *Colloid Polym. Sci.* **1990**, *268*, 885–894.
(16) Adedeji, A.; Jamieson, A. M.; Hudson, S. D. *Macromolecules* **1994**, *27*, 4018–4019.
(17) Adedeji, A.; Jamieson, A. M.; Hudson, S. D., to be published.
(18) Wang, Z. G.; Safran, S. A. *J. Phys. (France)* **1990**, *51*, 185–200.
(19) Sadron, C.; Gallot, B. *Makromol. Chem.* **1973**, *164*, 301–332.
(20) Israelchivili, J. N. In *Physics of Amphiphiles, Micelles, Vesicles and Microemulsions*; Degiorgio, V., Conti, M., Eds.; North-Holland: Amsterdam, The Netherlands, 1985; p 21.
(21) Tucker, P. S.; Barlow, J. W.; Paul, D. R. *Macromolecules* **1988**, *21*, 1678–1685.
(22) Hashimoto, T.; Kimishima, K.; Hasegawa, H. *Macromolecules* **1991**, *24*, 5704–5712.
(23) Lowenhaupt, B.; Steurer, A.; Hellmann, G. P. *Macromolecules* **1994**, *27*, 908–916.
(24) Leman, T., unpublished light scattering results (1994).
(25) Thomas, E. L.; Alward, D. B.; Kinning, D. J.; Martin, D. C.; Handling, D. L.; Fetters, L. J. *Macromolecules* **1986**, *19*, 2197.
(26) Folkes, M. J. *Processing, Structure and Properties of Block Copolymers*; Elsevier Applied Science Publishers Ltd.: England, 1985.
(27) Echte, A. *Angew. Makromol. Chem.* **1977**, *58/59*, 175–198.
(28) Utracki, L. A. *Polymer Alloys and Blends*; Hanser Publishers and Oxford Press: New York, 1989.
(29) Winey, K. I.; Thomas, E. L.; Fetters, L. J. *Macromolecules* **1992**, *25*, 2645–2650.
(30) Flory, P. J. *Statistical Mechanics of Chain Molecules*; Hanser Publishers: New York, 1989; Chapter 1, p 40.
(31) Tanaka, H.; Hasegawa, H.; Hashimoto, T. *Macromolecules* **1991**, *24*, 240–251.
(32) Adedeji, A.; Jamieson, A. M.; Hudson, S. D. *Polymer*, in press.
(33) Keskkula, H.; Turley, S. G.; Boyer, R. F. *J. Appl. Polym. Sci.* **1971**, *15*, 351–367.
(34) Jeon, H. G.; Hudson, S. D., unpublished result (1994).

MA9501609